**Supporting Information**

# A multisite-complexation-regulating solvent-dependent monomolecular chemosensor for quantifying $Fe^{3+}$/$ClO^-$ and fast detecting $Al^{3+}$/$Cr^{3+}$/$Cu^{2+}$

Wang Jiaojiao, GaoYanyan, Zhang Yuexing, Xu Dongmei, Li Zongxin, Su Yifei, Wang Fang, Zhang Ning, Zhang Daopeng, Wang Kang*, Chen Yuting*

# Content

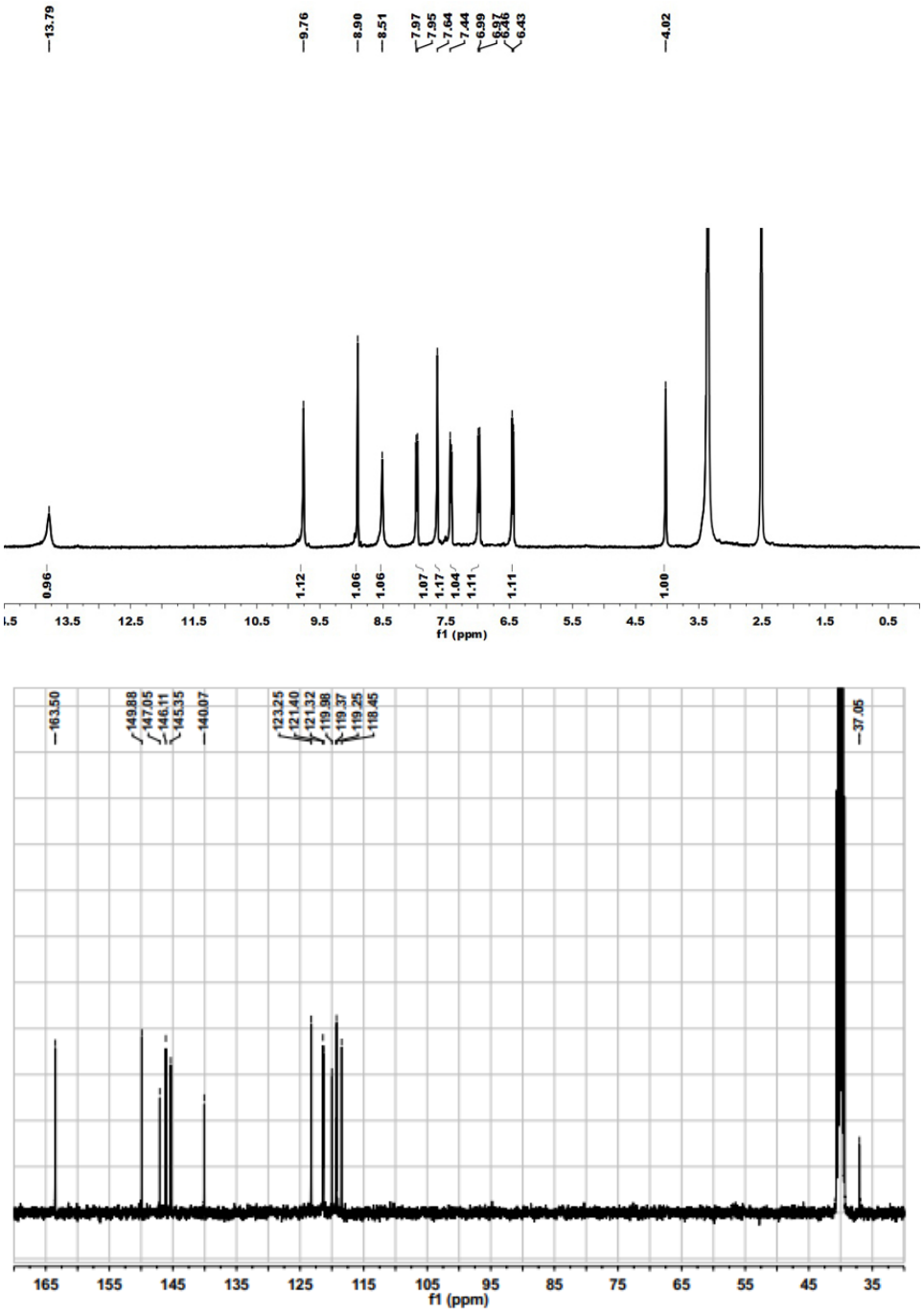


Fig. S1 The $^{1}H$ NMR and $^{13}C$ NMR spectra of DHSF in DMSO-$d_6$.

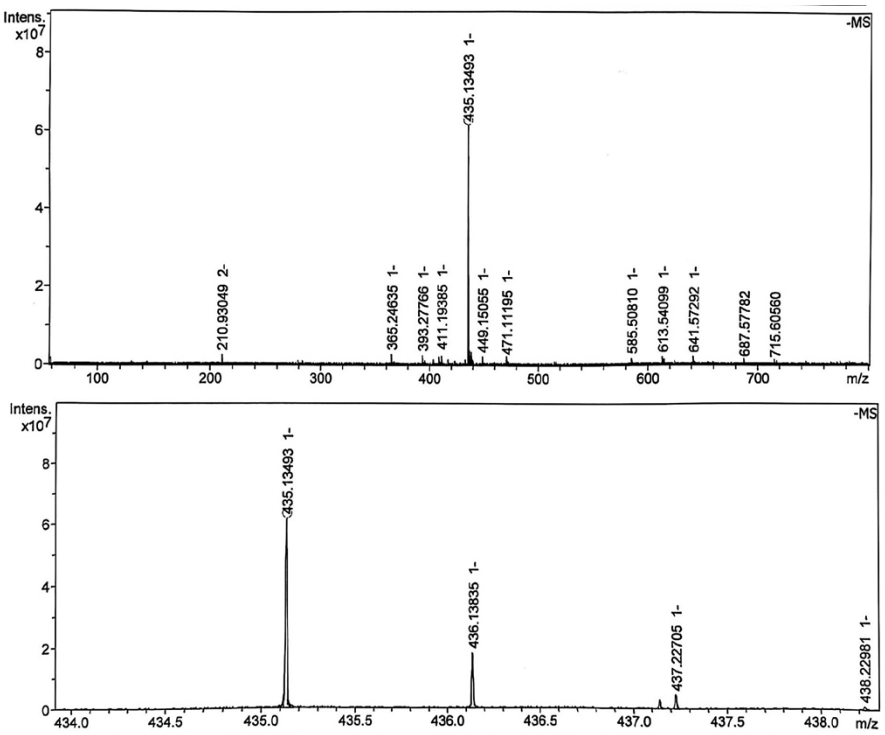


Fig. S2 The ESI-MS spectra of DHSF.

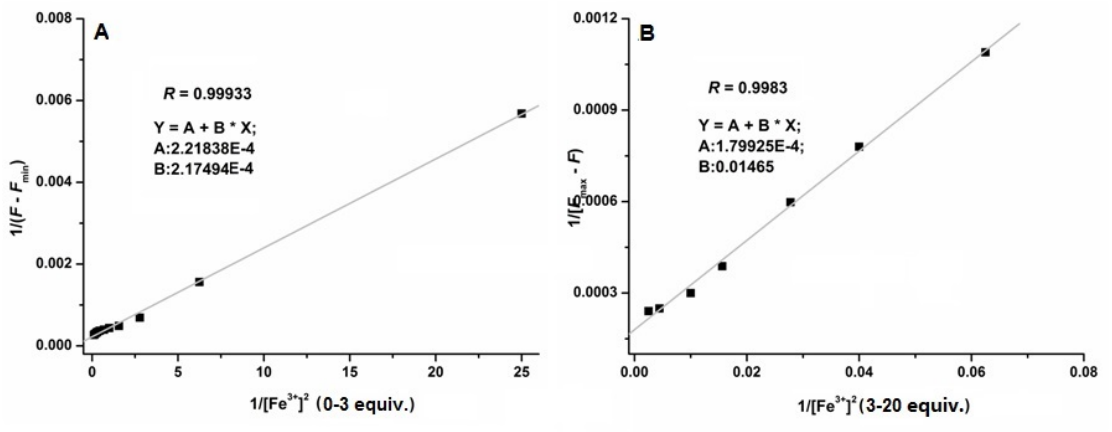


Fig. S3 The fluorescence linear change of DHSF (20 μM) with the increase of $Fe^{3+}$ amounts being 0-3 and 3-20 equiv. in a 5% $H_2O$-DMF mixed solvent, respectively.

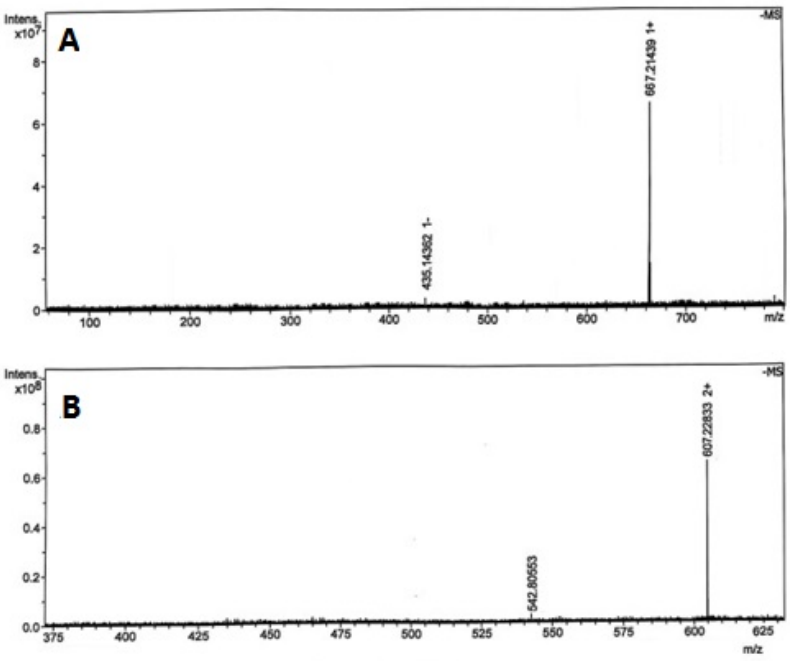


Fig. S4 ESI-MS spectra of DHSF upon addition of $Fe^{3+}$ with the different concentration being 3 (A) and 10 equiv. (B), respectively.

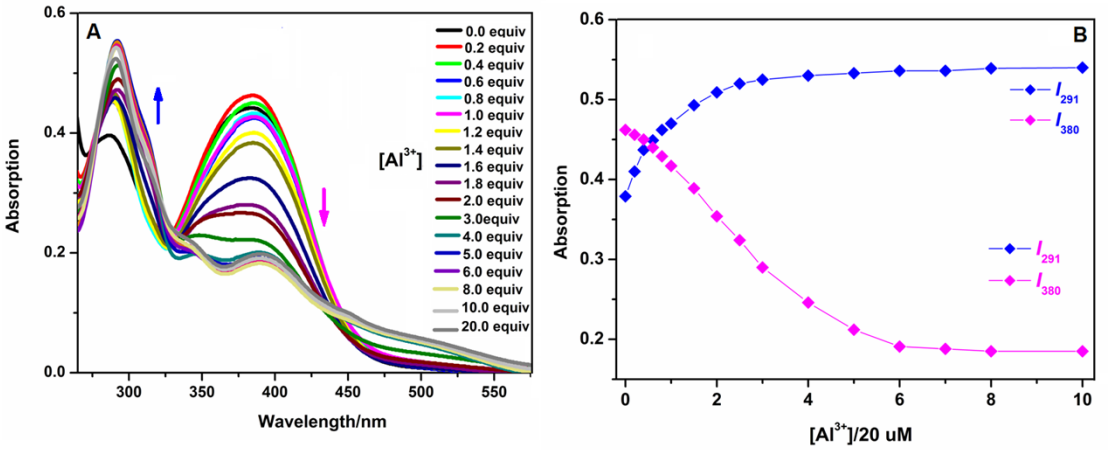


Fig. S5 The absorption spectra of DHSF (20 μM) upon increasing amount of $Al^{3+}$ from 0 to 20 equiv.

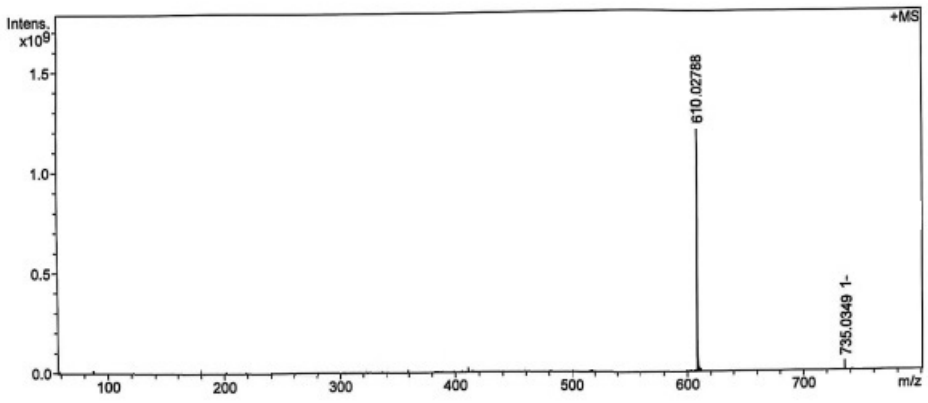


Fig. S6 ESI-MS spectra of DHSF upon addition of $Al^{3+}$.

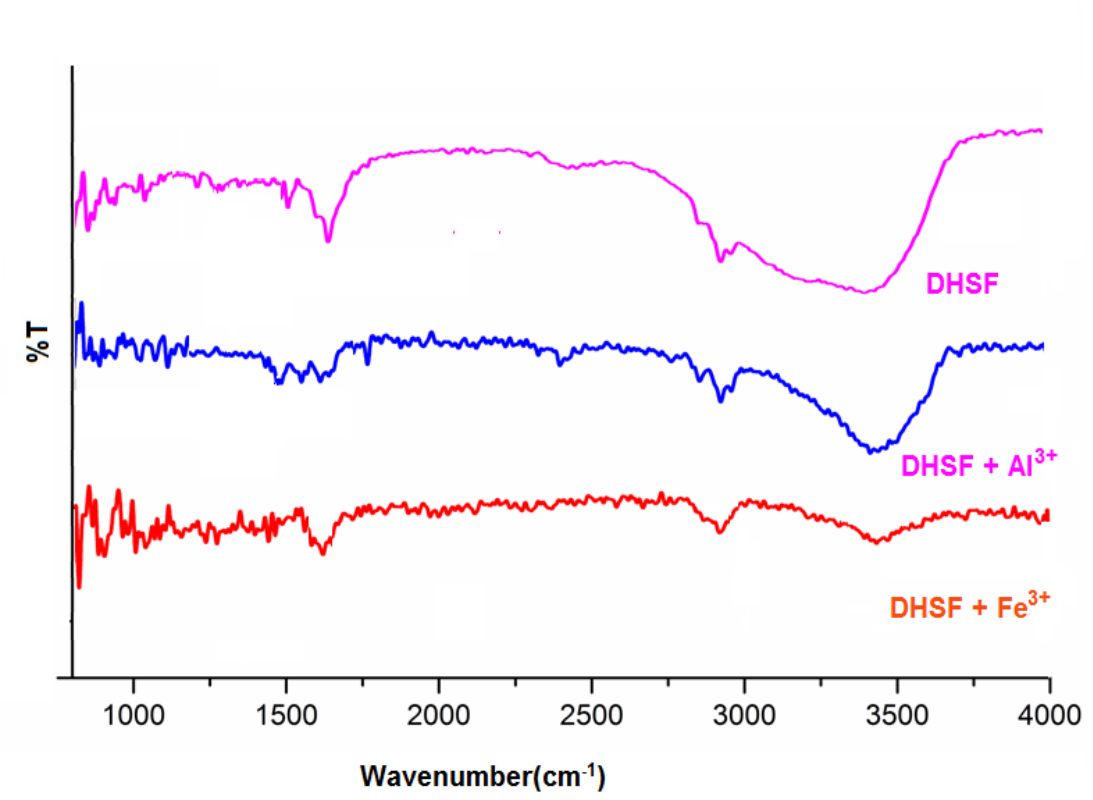


Fig. S7 The IR spectra for DHSF upon respective addition of $Al^{3+}$ and $Fe^{3+}$ (10 eqiuv.), respectively.

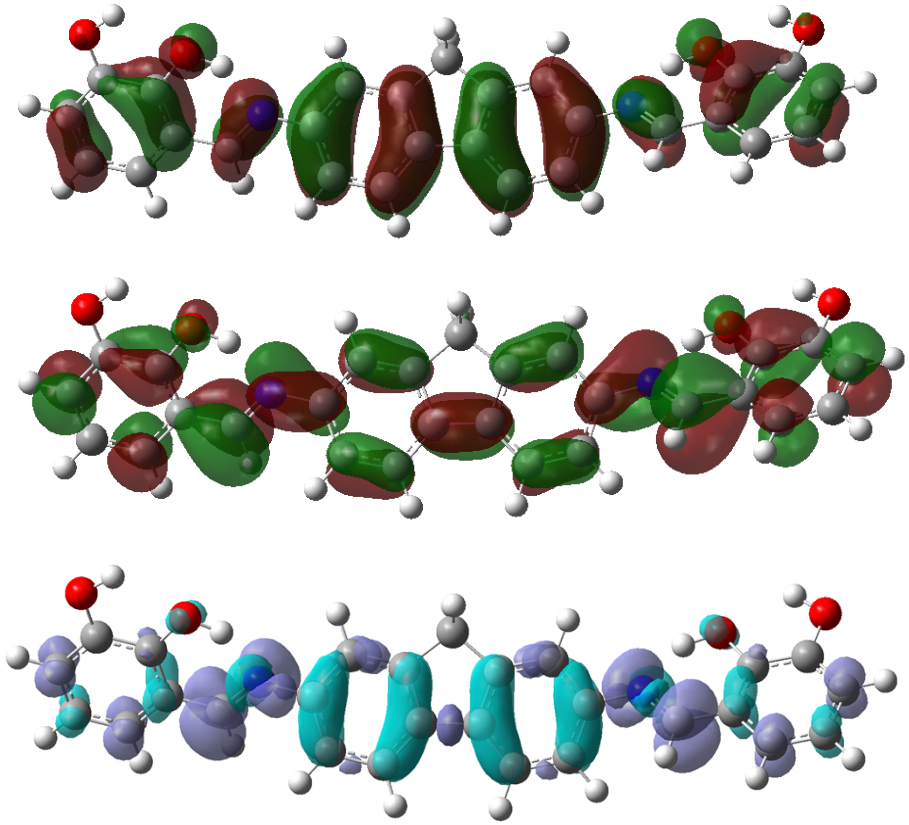

Fig. S8. The maps of the highest occupied molecular orbital (HOMO, top) and lowest unoccupied molecular orbital (LUMO, middle) as well as the charge transfer difference map for the lowest energy electronic absorption band (407.54 nm) (bottom) of DHSF1.

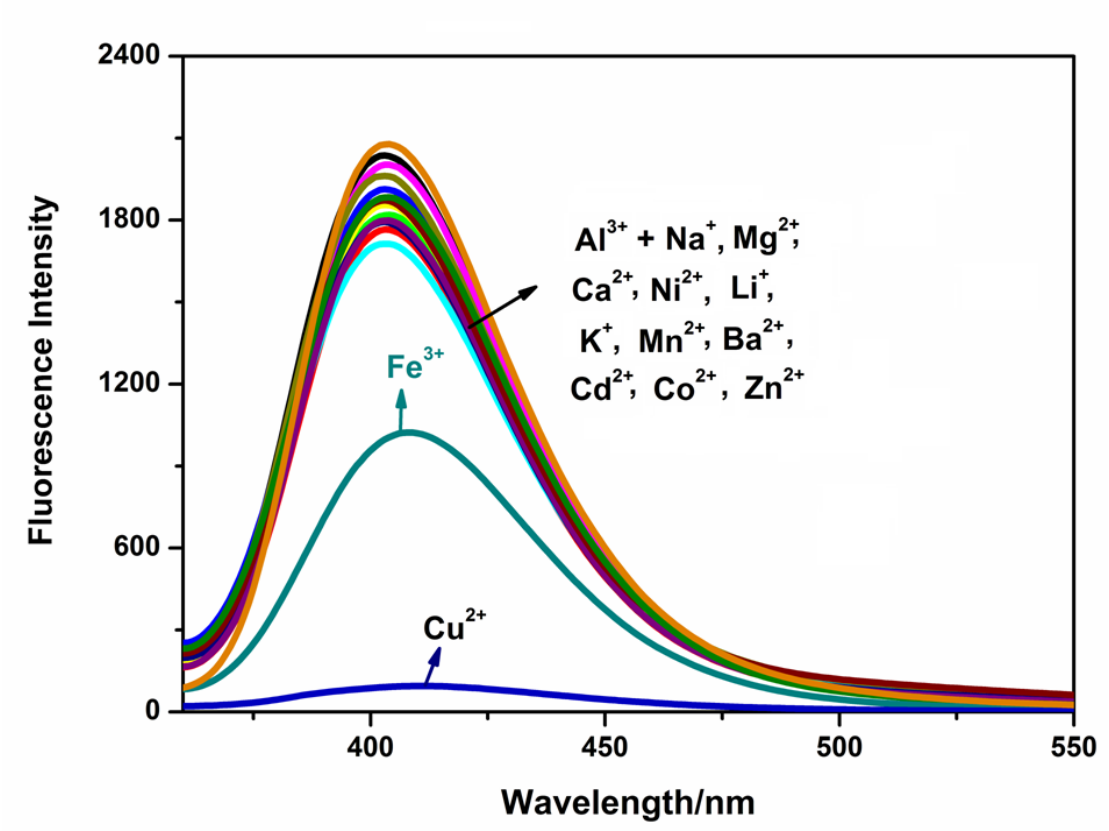


Fig. S9 The fluorescence emission spectra of DHSF-$Al^{3+}$ upon addition of other tested metal ions (1:10:10), respectively.

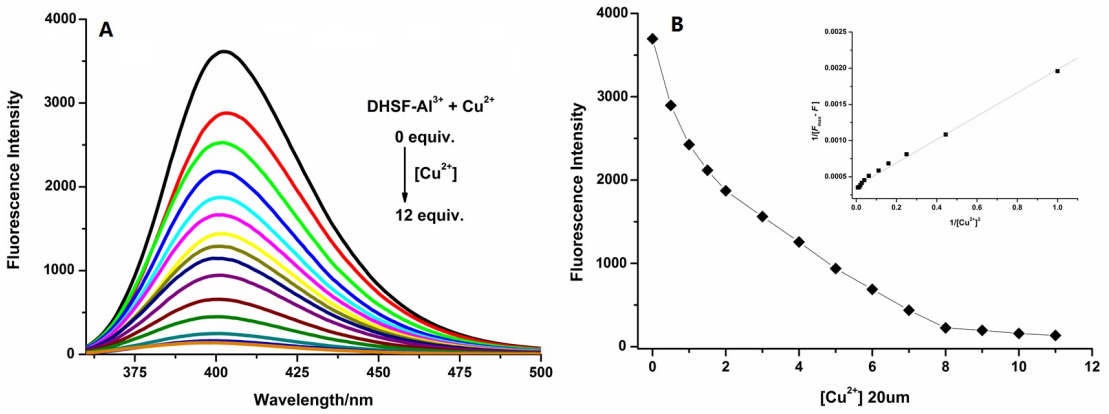


Fig. S10 The fluorescence titration experiment of DHSF-$Al^{3+}$ complex with $Cu^{2+}$, the inset in B showing the fluorescence linear change of DHSF-$Al^{3+}$ complex along with increasing $Cu^{2+}$ amounts on the basis of Benesi-Hildebrand in a 5% $H_2O$-DMF mixed solvent.

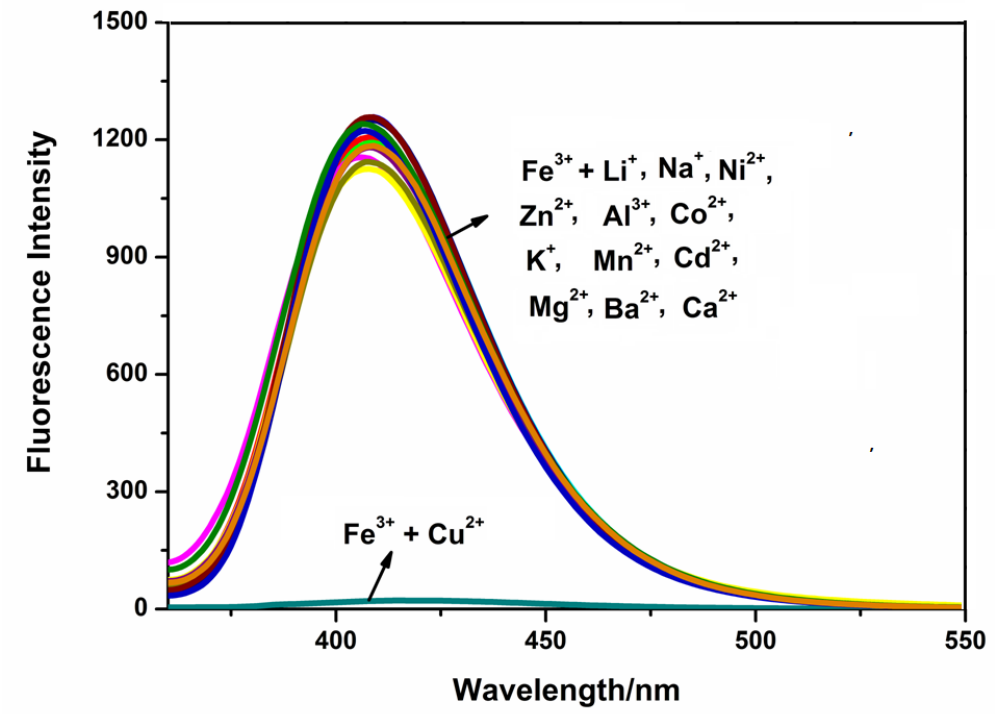


Fig. S11 The fluorescence emission spectra of DHSF-$Fe^{3+}$ upon addition of other tested metal ions (1:10:10), respectively.

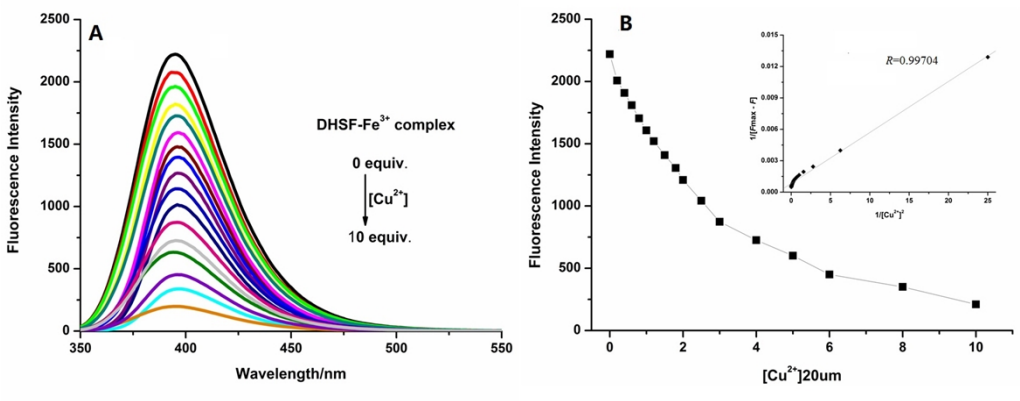


Fig. S12 The fluorescence titration experiment of DHSF-$Fe^{3+}$ complex with $Cu^{2+}$, the inset in B showing the fluorescence linear change of DHSF- $Fe^{3+}$ complex along with increasing $Cu^{2+}$ amounts on the basis of Benesi-Hildebrand in a 5% $H_2O$-DMF mixed solvent.

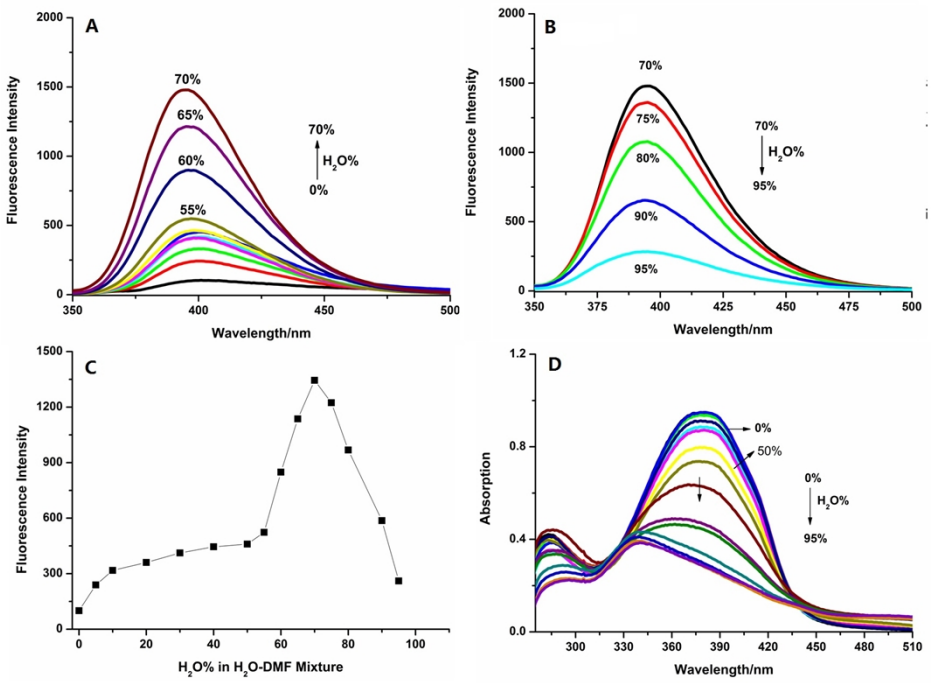


Fig. S13 The fluorescence emission (A, B, C) and electronic absorption (D) of DHSF in DMF-$H_2O$ mixture with $H_2O$ fractions ($f_w$) changing from 0 to 95%.

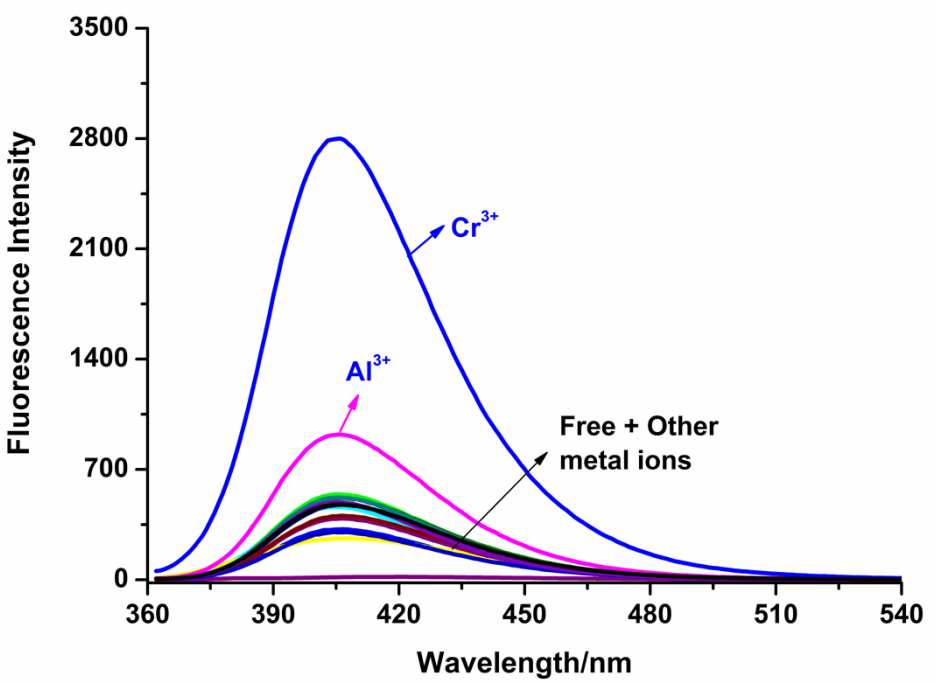


Fig. S14 Fluorescence emission of DHSF after adding different metal ions in a 50% $H_2O$-DMF mixed solvent.

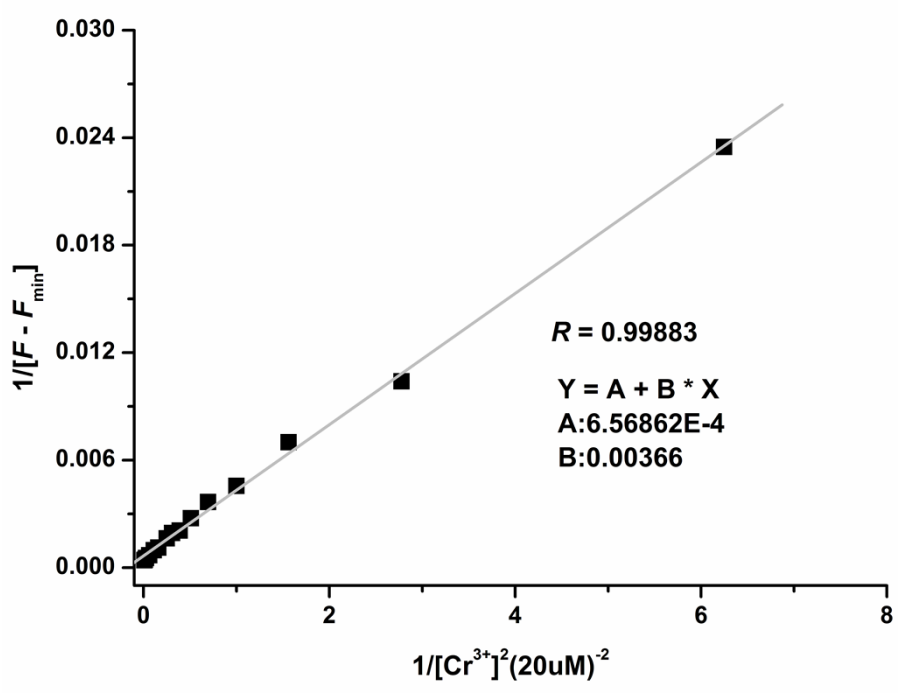


Fig. S15 The fluorescence linear change of DHSF with the increasing $Cr^{3+}$ amounts in a 50% $H_2O$-DMF mixed solvent.

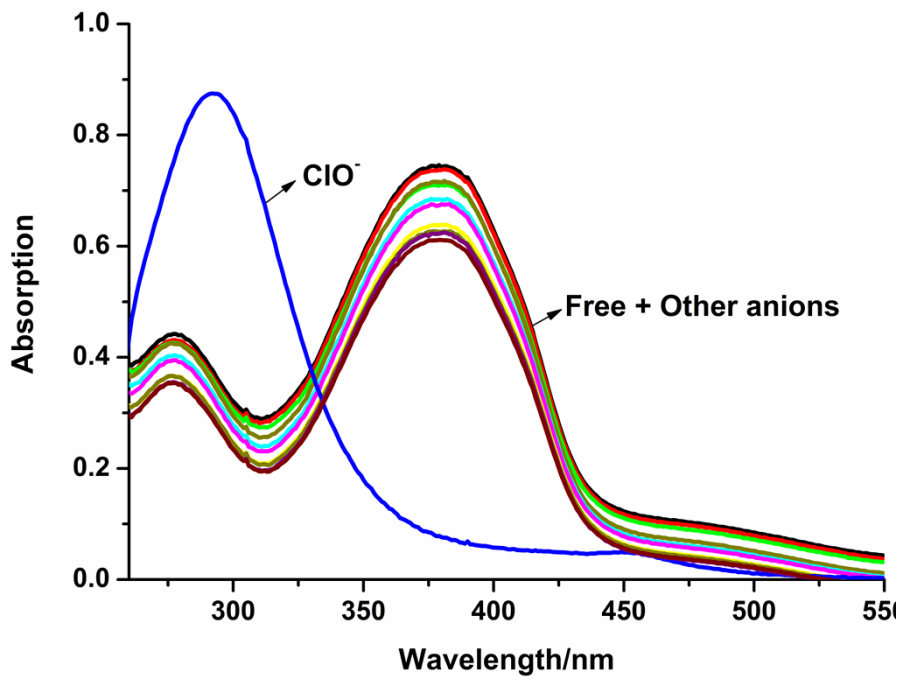


Fig. S16 The electronic absorption of DHSF after sodium salts with different anion were studied in 50% $H_2O$-DMF mixed solvent.

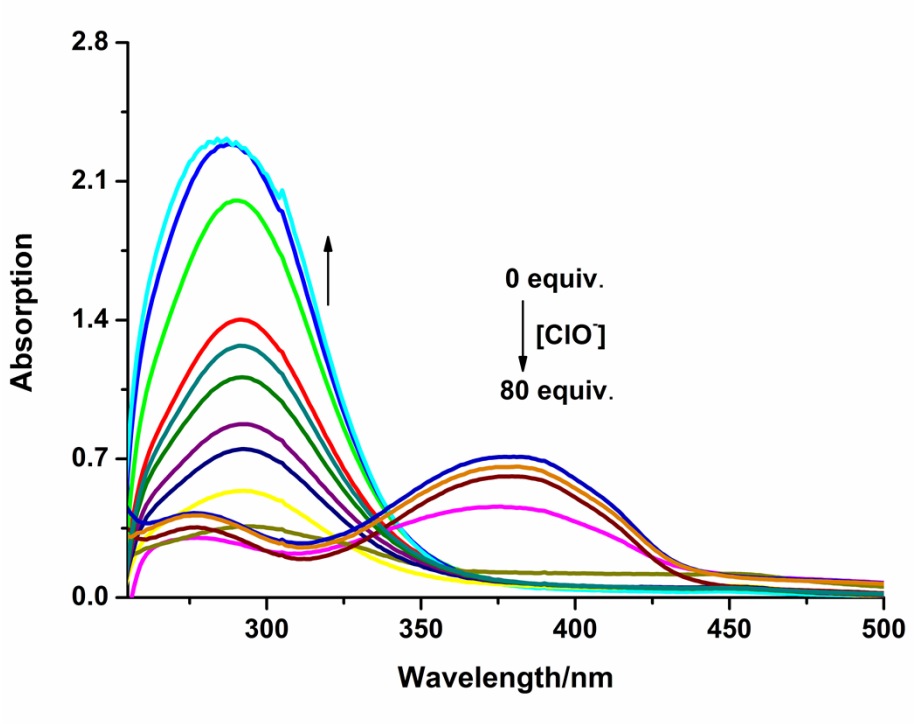


Fig. S17 The electronic absorption of DHSF along with the increasing amount of $ClO^-$ in 50% $H_2O$-DMF mixed solvent.

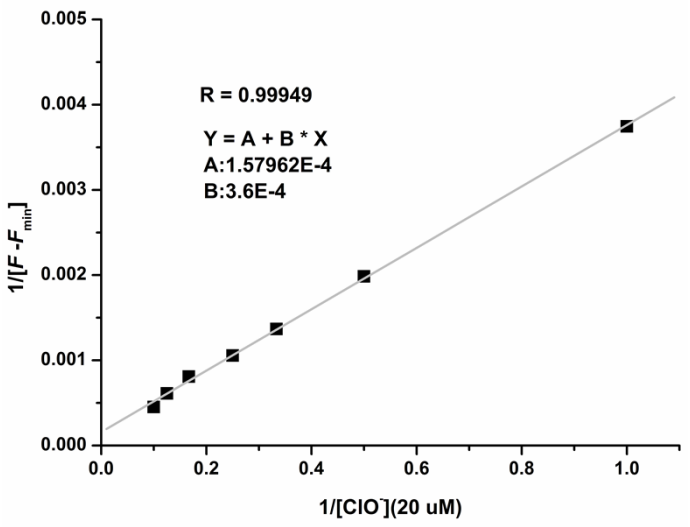


Fig. S18 The fluorescence linear change of DHSF with the increasing amount of $ClO^-$ in 50% $H_2O$-DMF.

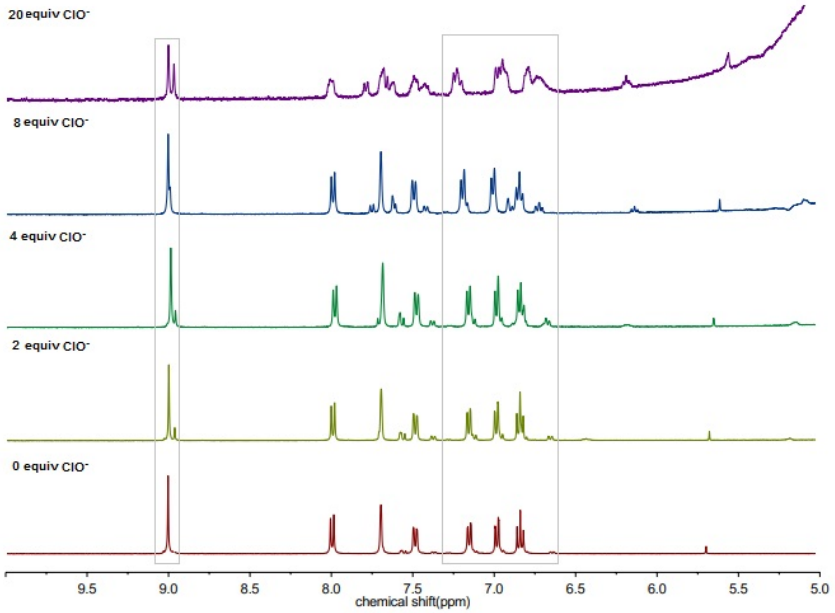


Fig. S19 The $^{1}H$ of DHSF upon addition of different $ClO^{-}$ amount.

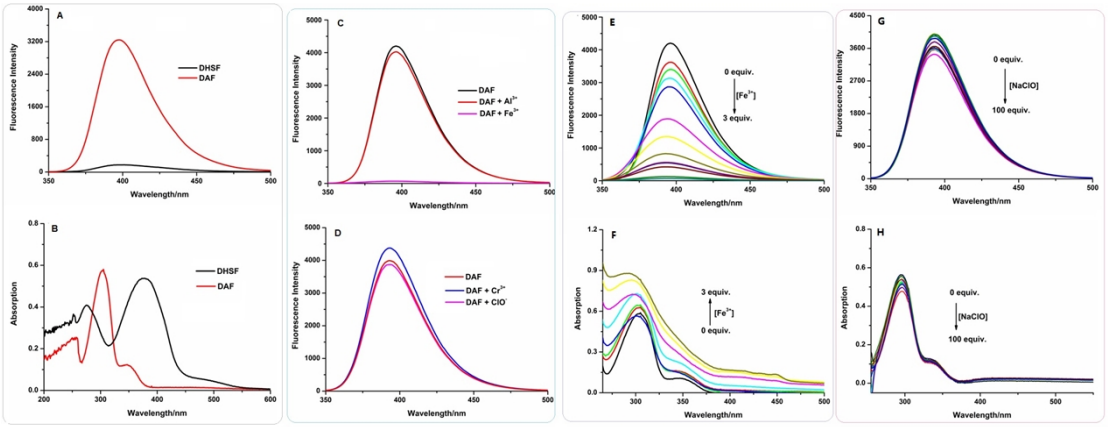


Fig. S20 The fluorescence emission (A) and electronic absorption spectra (B) of the reference DAF and DHSF; The fluorescence emission of DAF upon addition of $Al^{3+}$/$Fe^{3+}$ in 5% DMF-$H_2O$ (C) and $Cr^{3+}$/$ClO^-$ in 50% $H_2O$-DMF solvent (D), respectively; The fluorescence emission (E) and electronic absorption spectra (F) of DAF upon addition of different $Fe^{3+}$ amounts; The fluorescence emission (G) and electronic absorption spectra (H) of DAF upon addition of different $ClO^-$ amounts.

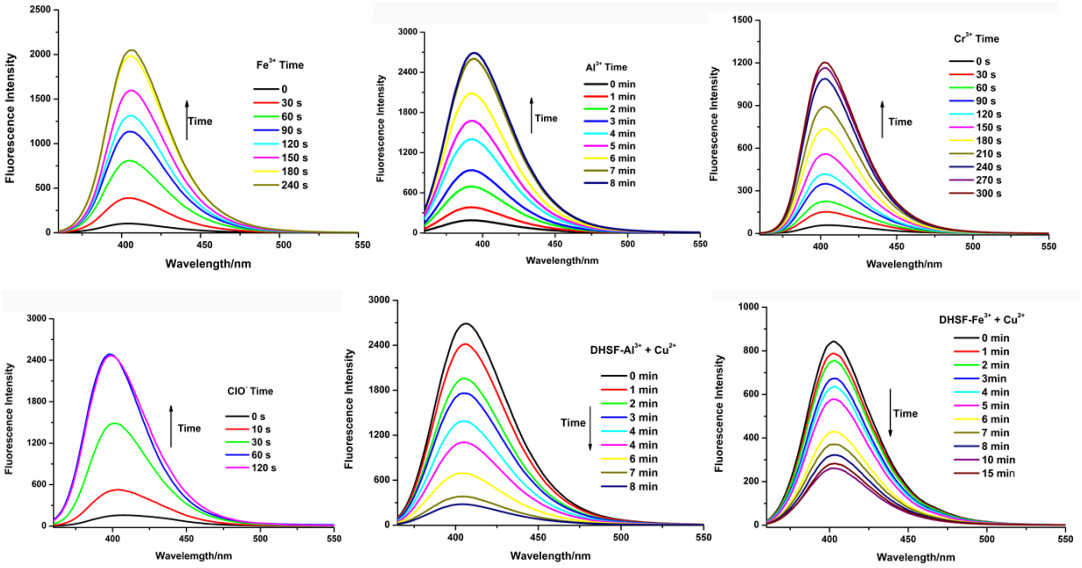


Fig. S21 The responsive times of DHSF towards $Fe^{3+}$, $Al^{3+}$, $Cr^{3+}$, $ClO^{-}$ and $Cu^{2+}$, respectively.

Table S1. Isomers of DHFS and relative electronic energy (in eV).

| Structures of different isomers | Relative energy (eV) |
|---|---|
| 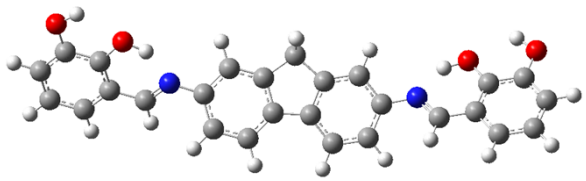 **DHFS1** | 0. 000 |
| 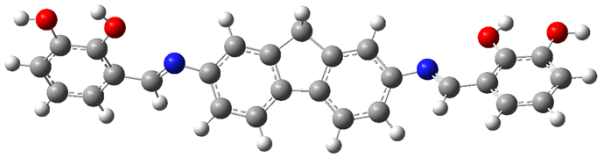 | 1. 230 |
| 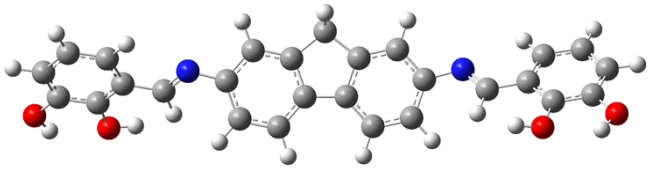 | 1. 042 |
| 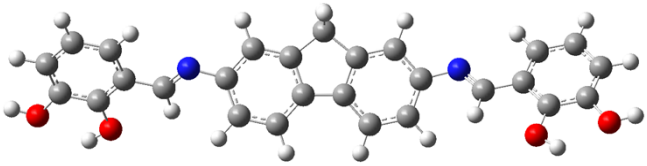 | 0. 880 |
| 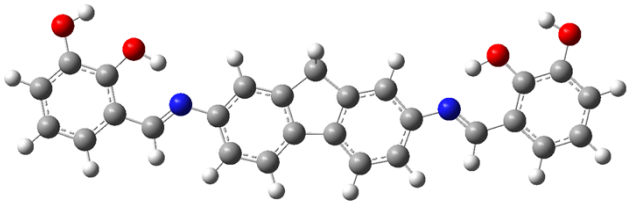 **Planar, C2V, -imaginary frequency of 37.5568 $cm^{-1}$** | 0. 063 |
| 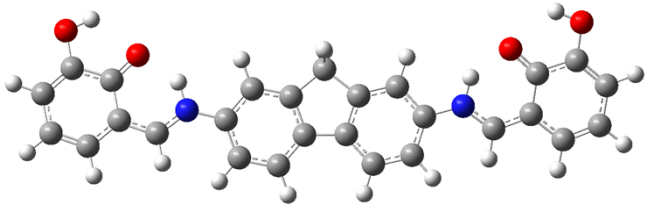 **DHSF2** | 0. 113 |
| 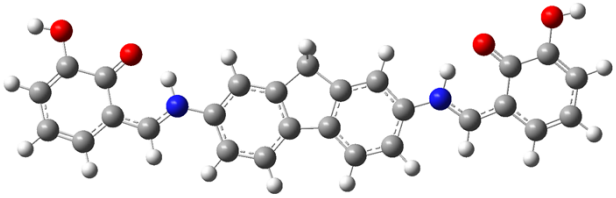 | 0. 829 |